Assessment of the mechanical integrity of silicon and diamond-like carbon coated silicon atomic force microscope probes

Jingjing Liu[a], David S. Grierson[a], Kumar Sridharan[a],
Robert W. Carpick[b], and Kevin T. Turner[a*]

[a]University of Wisconsin-Madison, 1513 University Ave., Madison, WI 53706
[b]University of Pennsylvania, 220 S. 33rd St., Philadelphia, PA 19104

ABSTRACT

The wear of atomic force microscope (AFM) tips is a critical issue in the performance of probe-based metrology and nanomanufacturing processes. In this work, diamond-like carbon (DLC) was coated on Si AFM tips using a plasma ion implantation and deposition process. The mechanical integrity of these DLC-coated tips was compared to that of uncoated silicon tips through systematic nanoscale wear testing over scan distances up to 0.5 meters. The wear tests consisted of a combination of contact-mode AFM scanning, transmission electron microscopy, and pull-off force measurements. Power spectral density analysis of AFM measurements acquired on structured samples was used to evaluate the imaging performance of the tips. The results show that Si tips are prone to catastrophic failure in self-mated contacts under typical scanning conditions. In contrast, DLC-coated tips demonstrate little to no measurable wear under adhesive forces alone, and exhibit stress-dependent gradual wear under external loads of ~22 and 43 nN.

1. INTRODUCTION

Atomic force microscopy (AFM) has become an indispensible tool in science and industry for high-resolution surface imaging, material property measurements, metrology, process control, and nanoscale manipulation. The sharpness and robustness of the probe tips are critical issues that control resolution and reliability in these applications. An ideal AFM tip is atomically sharp and mechanically robust, with a tunable surface chemistry. Silicon has been widely used as a tip material due to the maturity of microfabrication techniques adapted from the semiconductor industry. However, the modest strength, hydrophilicity of the native oxide surface, and low fracture toughness can lead to catastrophic failure of the probe tip. To push the limits of industrial AFM applications, there is a critical need to develop new tip materials and to understand how tip evolution affects AFM imaging resolution and material property measurements.

Diamond-like carbon (DLC) is known for its low macroscopic friction coefficient and chemical inertness, and has been routinely used as a wear-resistant coating in the automobile and hard-disk industry. A recent report shows that monolithic silicon DLC AFM tips, fabricated using a molding technique, have a wear resistance that is three orders of magnitude larger than that of silicon tips in ambient conditions [1]. The progress in batch fabrication of carbon-based AFM tips may soon lead to the development of AFM applications that require long scanning times, such as high-throughput imaging, local electrical characterization for process control in micro/nanoelectronics, nanomechanical characterization of MEMS/NEMS devices [2, 3], nanolithography [4-6], and massively-parallel AFM-based arrays for nanomechanical data storage at ultrahigh density [1, 7].

In this paper, commercial high aspect ratio Si tips were coated with DLC films, and the imaging performance of the DLC-coated tips and uncoated Si tips was investigated by conducting self-mated AFM wear scans over a scan distance up to 0.5 m. The degradation of image resolution is evaluated, and the effect of normal contact stresses on tip wear/failure is examined.

* Prof. Kevin T. Turner, kturner@engr.wisc.edu, tel: 608.890.0913

Instrumentation, Metrology, and Standards for Nanomanufacturing IV, edited by Michael T. Postek, John A. Allgair,
Proc. of SPIE Vol. 7767, 776708 · © 2010 SPIE · CCC code: 0277-786X/10/$18 · doi: 10.1117/12.861789

2. METHODS

2.1 DLC coating

Beginning with commercial single crystalline Si probes (NanoSensors^{TM}), DLC films were deposited by a plasma immersion ion implantation and deposition (PIIID) process using an acetylene plasma at a pressure of 12 mTorr and a 5kV applied bias. The plasma was created using the glow discharge method. The films had an intended thickness of 20 nm based on known growth rates of the DLC using this process. The PIIID process is non-line-of-sight in nature and allows for uniform coating of complex 3D geometries [8].

2.2 Wear characterization

The wear properties of the DLC-coated tips and Si tips were systematically characterized using a wear test protocol consisting of a combination of contact-mode AFM scanning, transmission electron microscopy (TEM) imaging, and pull-off force measurements (see ref. [9] for a detailed description of the methodology). The DLC-coated tips ("D") and Si tips ("S") with a native oxide were scanned on a DLC-coated Si substrate ("D") and a thermally-oxidized Si substrate "(S)", respectively, to form self-mated contacts. We refer to tips from these experiments as "DD" and "SS", to indicate the tip and the sample material respectively. Experiments consisting of DS and SD interfaces have also been conducted, and those results will be published elsewhere. Both substrates have nominally the same smoothness (RMS roughness < 2 nm over a 1x1 μm^2 area). Each wear test consists of acquiring a total of 100 contact-mode images (5×5 μm^2 area each, obtained by raster scanning with 512 lines per image) using a Veeco MultiMode AFM. The scans were conducted in a controlled environment (13% relative humidity (RH) in a nitrogen background) and with zero externally applied load for both types of tips. Thus, the only normal load acting is due to interfacial adhesion. Higher applied loads were applied when testing two of the DLC-coated tips to create more aggressive wear conditions. After the 1st, 5th, 10th, and every 10th image thereafter, pull-off forces (also called force-distance curves) were measured to monitor the adhesive forces between the tip and sample, as well as to readjust the applied load to the desired level. Additionally, after each period of pull-off force measurements, the tips were used to image a Nioprobe® sample (1×1 μm^2 area), which is a commercial tip characterization surface (MikroMasch, San Jose, CA) with sharp features that enable evaluation of the imaging performance and tip geometry throughout the wear test. Finally, structural and morphological changes of the tip were imaged using transmission electron microscopy (TEM) (JEOL 100CX TEM) periodically during the test.

2.3 AFM image resolution

The Nioprobe® surface consists of sharp spikes with radii of curvature of less than 5 nm. The AFM image of any surface is a convolution of the tip geometry and the surface features; therefore, when the tip size is larger than the Nioprobe spikes, the image of the surface is essentially consists of repeated inverse images of the tip. Thus, Nioprobe® images provide information about the tip geometry and therefore the imaging capability of the tip. However, unlike 2-dimensional imaging in optics, there is no well-accepted definition for resolution for 3-dimensional topographic images. One way to assess changes in image resolution is to calculate power spectral densities (PSDs) and compare them among images acquired with tips with different shapes and/or sizes. PSDs are widely used in spectrum analysis and surface roughness assessment. To calculate a PSD spectrum, a given line profile from an AFM image is treated as a signal. The Fourier transform of the profile is taken, squared, and normalized by the spatial frequency, thereby producing the PSD. PSD spectra are typically plotted as a function of spatial frequency (*e.g.*, 1/μm), with the intensity of the PSD spectrum at a specific frequency corresponding to the amplitude of the component at that frequency. Thus, the relative intensity of a PSD spectrum at a given frequency reflects the relative contribution of the corresponding frequency component to the total signal. For evaluating the resolution achieved by an AFM tip used to generate an AFM image, the PSD spectrum is a quantitative measure of the tip's ability to resolve features over a range of spatial frequencies. In particular, comparing PSD spectra achieved with the same tip at various stages of wear can provide insight into the connection between changes in tip shape and changes in imaging resolution. In some cases, when the worn tip becomes 'squared-off', interpretation of the PSD spectrum becomes more complicated (due to the addition of higher-frequency components caused by the sharp corners), and establishing a correlation between the PSD intensities and the resolved feature sizes requires additional analysis (this will be discussed in future publications). Since each AFM image is acquired with raster scanning, the amount of noise in the fast-scan direction (*x*-direction, perpendicular to the long axis of the cantilever) and slow-scan direction (*y*-direction, parallel to the long axis of the cantilever) are different. To avoid the additional noise

present in the slow-scan direction due to line-by-line variations, we report only PSD spectra taken along the slow-scan direction (*x*-direction). The PSDs along lines of data in the *x*-direction were calculated using the "pwelch" function in Matlab® (MathWorks, Natick, MA) and then averaged.

2.4 Adhesion and contact stress analysis

The adhesive force between a tip and a substrate is a function of the tip geometry and the work of adhesion (W) between the tip and surface. In Derjaguin-Müller-Toporov (DMT) regime [10], which applies to stiff materials with weak, long-range adhesion, and a small tip radius, the adhesive force (F_{ad}) of a paraboloidal tip with radius of curvature R on a flat surface is

$$F_{ad} = 2\pi WR\,. \tag{1}$$

With a tip of known radius, pull-off force measurements can therefore be used to determine the work of adhesion. If the tip radius is unknown, a change in the measured F_{ad} reflects either a change in surface chemistry (through the work of adhesion W) or tip geometry. The DMT model treats the adhesive force simply as an additional normal load, and assumes the whole system obeys Hertzian contact mechanics [11]. The DMT contact radius, a, can be expressed as:

$$a = \left(\frac{R}{K}\left(F + F_{ad}\right) \right)^{1/3} \tag{2}$$

where F is the applied load, and

$$K = \frac{4}{3}\left(\frac{1-\nu_1^2}{E_1} + \frac{1-\nu_2^2}{E_2} \right)^{-1} \tag{3}$$

with E_1, E_2 being the tip and surface Young's moduli, respectively, and ν_1, ν_2 being the Poisson's ratios of the tip and surface, respectively. If the apex of a tip becomes flattened due to wear, the tip geometry can, in general, be better described by a power-law function than by a paraboloid [12]:

$$z = \frac{x^n}{nQ} \tag{4}$$

where n is the power index, and Q is the radius of curvature of the n^{th} order with the units of m^{n-1}[12-14]. When n=2, the power-law function reduces to a parabolic shape. The adhesive force for a power-law shaped tip in the DMT limit can be written as [12]:

$$F_{ad} = \frac{W}{h}\pi(nhQ)^{\frac{2}{n}} \tag{5}$$

where h is the adhesion range in the Dugdale approximation for the adhesive interaction [15]. The contact radius can be derived from Hertzian contact mechanics equations [15], and is expressed as follows:

$$a = \left(\frac{4(F + F_{ad})Q}{3K\sqrt{\pi}} \frac{\Gamma(\frac{3+n}{2})}{\Gamma(\frac{2+n}{2})} \right)^{\frac{1}{n+1}} \tag{6}$$

where Γ is the gamma function. The average contact stress in a tip-sample contact can be calculated by dividing the total load ($F + F_{ad}$) by the contact area ($2\pi a^2$).

3. RESULTS AND DISCUSSION

3.1 AFM image resolution

The 1×1 μm^2 AFM images of the Nioprobe® surface for the DLC-coated tip (DD-1) and Si tip (SS-1) at different stages in the wear testing under adhesive forces alone are shown in Figure 1. The DLC-coated tip resolves consistent feature sizes before wear scanning, after scanning 20 images, and after scanning 100 images. In contrast, the Si tip is sharper than the DLC-coated tip initially (Figure 1(a)), but changes drastically immediately after the first 5×5 μm^2 scan on the SiO_2 surface (Figure 1 (c, d)). Instead of the high aspect ratio protrusions seen before scanning, the image contains large triangular features which correspond to the cross-section of the broken Si tip, indicative of a large amount of volume removed due to tip fracture during the first scan image. Since the DLC-coated tip does not show a detectible change over the course of 100 scans at zero applied load, two further wear tests were performed under higher external loads. The higher loads were chosen to be approximately 5 times (test DD-L1 – applied load is) and 10 times (DD-L2) the initial DLC-on-DLC measured adhesive forces. The adhesive forces and external loads for all four tips tested are summarized in Table 1. The AFM images of the Nioprobe® sample from those two tips before and after 100 wear scans are compared with the images acquired with the DLC tip scanned under zero external load in Figure 2. Both DLC-coated tips scanned at higher loads showed a decrease in resolution at scan 100 as indicated by the larger circular features in the images of the Nioprobe® sample in Figure 2(d) and (f).

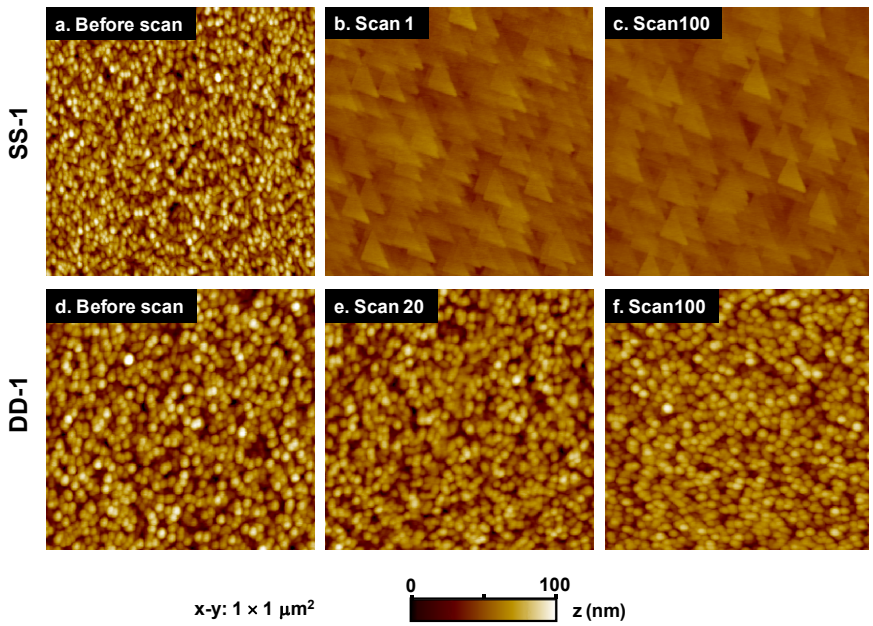

Figure 1. AFM topography images of a Nioprobe® sample acquired with a Si tip (a)-(c) and a DLC-coated tip (d)-(f) over the course of the wear test.

PSD spectra of the Nioprobe® images taken by the Si and DLC tips are shown in Figure 3. The spatial frequencies of 1 μm^{-1} and 256 μm^{-1} correspond to wavelengths of 1 μm (the width of the image) and 1.95 nm (the width of two pixels), respectively. PSDs with higher intensities at higher spatial frequencies indicate that smaller features were able to be resolved by the AFM tip. As shown in the PSD spectra acquired from the Nioprobe® surfaces scanned with the Si tip, the intensities of all frequency components drop drastically after the first image was acquired, and then are relatively constantly over the remainder of the test (Figure 3(b)). The PSD spectra from the DLC tip tested under zero applied load show minor changes over the course of the wear test, with only a slight reduction in intensity observed in the 10-40 nm wavelength range. However, significant intensity reductions in the PSD spectra are seen for the DLC tips scanned with external loads (DD-L2 and DD-L1). The PSD spectra from the DLC tip scanned under a higher external load (DD-L2) show a monotonic reduction in intensity for all spatial frequencies (Figure 3 (c, d)) as the wear test progressed. The DLC tip under lower load (DD-L1) has smaller but more complicated changes and only shows significant decreases in power spectral density at low spatial frequencies. The behavior observed in this PSD is currently under investigation. Overall, the agreement between the qualitative

Table 1. Summary of forces, tip radius, and work of adhesion prior to scanning.

Test	External Load (nN)	Adhesive Force (nN)	Initial Tip Radius (nm)	Work of adhesion (mJ/m^2)
SS-1	--	16±2.7	15.5±0.26	150±23
DD-1	--	5±0.6	27.7±0.02	26±4
DD-L1	22	3±1.5	21.9±0.12	23±14
DD-L2	43	5±1.7	27.7±0.16	28±9

assessments of the Nioprobe® images is good and the quantitative trends observed in the PSD spectra highlight the utility of PSDs for assessing the resolving capability of AFM tips.

3.2 Tip failure and pull-off force analysis

TEM images of the Si and DLC-coated tips taken at different stages of the wear testing are shown in Figure 4, revealing the origin of the decrease in resolution observed in the Nioprobe® images. The Si tip was initially sharp, but the TEM shows that the tip apex was completely removed after acquiring the first 5×5 μm^2 image with the tip. This large change in tip geometry is reflected in the Nioprobe® AFM images and PSD spectra. Small bumps and crevices can be observed on the sides of the initial Si tip in the TEM image. These features are due to the reactive ion etching (RIE) process used to form the tip, and they likely act as stress raisers when the tip experiences loading. These stress concentrators can act as fracture initiation points, leading to fracture of the tip. The DLC tip loaded by adhesive forces alone has no detectable changes in tip geometry in Figure 4, in agreement with the AFM images in Figure 2 (a, b). The DLC tip scanned with an applied external load of ~43 nN shows a gradual change in tip geometry (Figure 4 (d)-(i)), consistent with the AFM images shown in Figure 2 (e, f). Tip profiles were extracted from the TEM images and fit with power-law functions (Eq. (4)) to allow for the work of adhesion to be determined from measured pull-off forces using the analysis in Section 2.4. Finally, note in Figure 4 that the thickness of the DLC coatings is seen to be approximately 20 nm, as expected based on deposition conditions.

The pull-off forces measured for the four tips over the course of the 100 wear scans in each test are plotted in Figure 5. The work of adhesion between each tip-sample contact was calculated from the pull-off forces measured before any scanning using Eq. (1) and are listed in Table 1. Looking carefully at the Si pull-off force *versus* scan distance data, there is a peak pull-off force immediately after scan 1, and the pull-off force drops and stays constant thereafter. The TEM images reveal no detectible geometric changes of the Si tip between scan 1 and scan 100. Therefore, the high pull-off force measured immediately after scan 1 is likely caused by an increase in both the contact area and the work of adhesion, with the work of adhesion

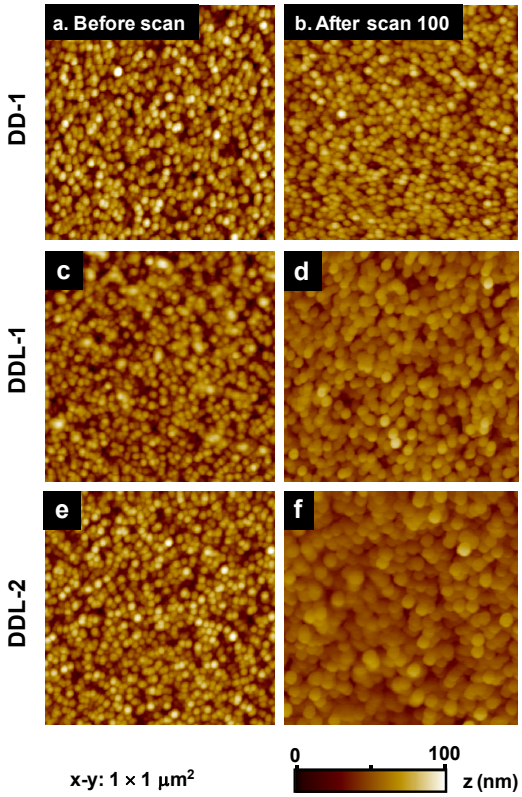

Figure 2. AFM topography images of a Nioprobe® sample acquired with three different DLC-coated tips before and after scanning the tips ~512 mm on DLC a surface under zero external load (a, b), an applied load of ~22 nN (c,d), and an applied load of ~43 nN (e,f).

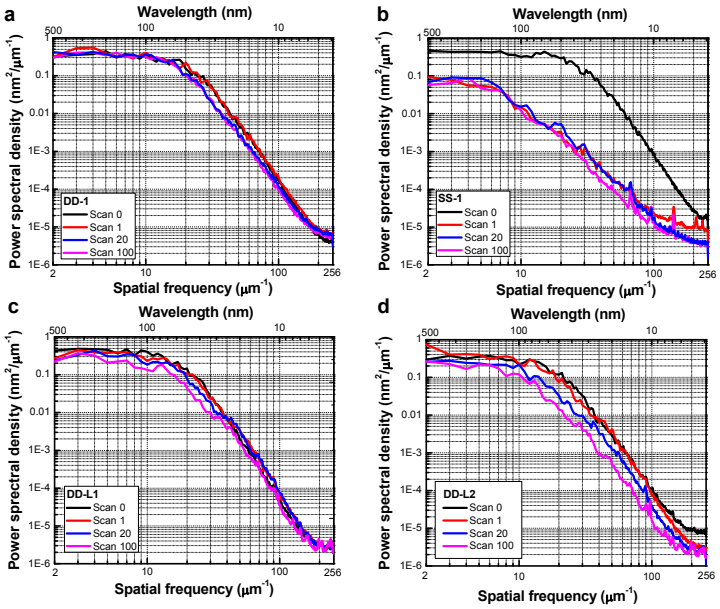

Figure 3. PSD spectra of the Nioprobe® AFM images obtained by a Si tip and three DLC tips at various stages during wear testing: (a) DD-1, (b) SS-1, (c) DD-L1, (d) DD-L2.

increase being due to dangling bonds and/or poorly-formed oxide present on the newly-fractured Si surface. The DLC tip tested under zero external load (DD-1) shows a constant pull-off force over the entire test, which is consistent with the TEM and AFM images that showed minimal changes during the wear testing. Increases in pull-off force with scan distance were measured for the DLC tips scanned under externally-applied loads (DD-L1 and DD-L2), which is consistent with the evolution observed in both the TEM and AFM images.

From the measured tip geometries, adhesive forces, and applied loads, the average (compressive) contact stresses for all four tips were calculated using Eq. (2) and Eq. (6). Note, in these calculations we treat the DLC tip as a monolithic entity and do not consider the finite thickness of the coating. Since the contact stresses decrease significantly within ~10 nm (related to the contact radius) of the surface and the coating thickness is approximately 20nm, we do not expect this simplification to affect the stress estimates significantly. Table 2 presents comparisons between initial average contact stresses and contact stresses calculated over the course of the wear tests. The DLC tip that is subjected to no externally applied load experiences a moderate stress level of ~4.6 GPa and retains it shape during the ~512 mm scan distance. The two tips scanned under higher external loads experienced higher stresses initially. For both tips, the stress levels decreased as the tips became blunter due to wear. Clearly, higher stresses correlate with more dramatic changes in tip geometry (Figure 2 and Figure 3), Interestingly, suggesting that the process of tip wear leading to a reduced stress. This suggests that the steady-state geometry of the tips may be largely determined by the allowable compressive stress that the DLC can withstand. Note that our stress analysis assumes that continuum mechanics is valid, assumes that the surfaces are perfectly smooth, and ignores the effect of the interfacial shear stress developed due to frictional sliding. Ongoing efforts seek to address these limitations.

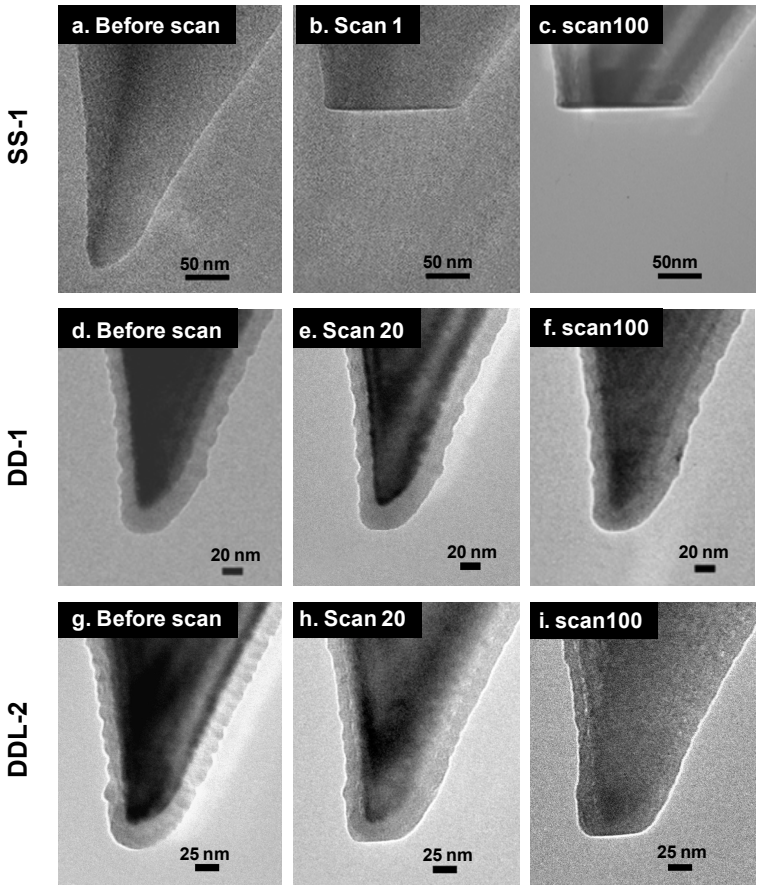

Figure 4. TEM images of three of the tips that were characterized after various numbers of AFM scans with the tips.

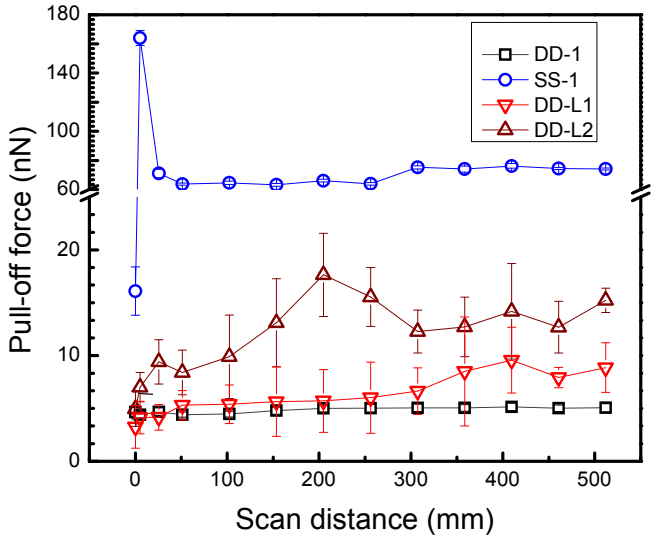

Figure 5. Pull-off force versus scan distance for a Si tip and the three DLC-coated tips.

Table 2. Average contact stress in the tip sample contact during the wear test

	SS-1(GPa)	DD-1(GPa)	DD-L1(GPa)	DD-L2(GPa)
Scan 0/Distance ~0 mm	13.1	4.7	15.7	22.4
Scan 1/Distance ~5.1 mm	1.7	*	*	*
Scan 5/Distance ~25.6 mm	*	*	3.9	8.6
Scan 20/Distance ~102 mm	*	4.5	3.7	5.2
Scan 100/Distance ~512 mm	1.7	5.1	2.6	3.7

*TEM images were not taken at these scan distances and therefore contact areas could not be estimated

4. CONCLUSIONS

The imaging performance of Si and DLC-coated Si tips was studied using a systematic AFM wear test protocol that included continuous self-mated wear scans using an AFM and regular tip characterization by TEM and pull-off force measurements. Under zero external load, which is typical in contact mode AFM imaging, the results show that a DLC tip has superior wear resistance compared to a Si tip in dry conditions (13% RH in N_2). The Si tip experienced catastrophic failure in a scan distance of only ~5 mm, while the DLC tip retained its initial geometry over the entire distance of the test (~512 mm). Gradual tip wear is observed for DLC tips scanned under higher external load and a dependence of the wear rate on the normal stress in the tip-sample contact is observed. Observations of changes in tip geometry and resolution loss in AFM images on tip characterization samples, PSDs, TEM, and pull-off forces agree.

REFERENCES

[1] H. Bhaskaran, B. Gotsmann, A. Sebastian *et al.*, "Ultralow nanoscale wear through atom-by-atom attrition in silicon-containing diamond-like carbon," Nature Nanotechnology, 5(3), 181-185 (2010).

[2] O. M. El Rifai, B. D. Aumond, and K. Youcef-Toumi, "Imaging at the nano-scale," Proceedings 2003 IEEE/ASME International Conference on Advanced Intelligent Mechatronics. 2, 715-22.

[3] A. Yacoot, and L. Koenders, "Aspects of scanning force microscope probes and their effects on dimensional measurement," Journal of Physics D: Applied Physics, 41(10), 103001 (46 pp.) (2008).

[4] A. J. M. Giesbers, U. Zeitler, S. Neubeck *et al.*, "Nanolithography and manipulation of graphene using an atomic force microscope," Solid State Communications, 147(9-10), 366-9 (2008).

[5] D. Bullen, X. Wang, J. Zou *et al.*, "Design, fabrication, and characterization of thermally actuated probe arrays for Dip Pen nanolithography," Journal of Microelectromechanical Systems, 13(4), 594-602 (2004).

[6] A. J. Senesi, D. I. Rozkiewicz, D. N. Reinhoudt *et al.*, "Agarose-assisted dip-pen nanolithography of oligonucleotides and proteins," ACS Nano, 3(8), 2394-2402 (2009).

[7] P. Vettiger, G. Cross, M. Despont *et al.*, "The "millipede"-nanotechnology entering data storage," IEEE Transactions on Nanotechnology, 1(1), 39-54 (2002).

[8] J. A. Bares, A. V. Sumant, D. S. Grierson *et al.*, "Small amplitude reciprocating wear performance of diamond-like carbon films: dependence of film composition and counterface material," Tribology Letters, 27, 79-88 (2007).

[9] J. Liu, J. Notbohm, R. W. Carpick *et al.*, "Method for Characterizing Nanoscale Wear of Atomic Force Microscope Tips," ACS Nano, doi: 10.1021/nn100246g, (2010).

[10] B. V. Derjaguin, V. M. Muller, and Y. P. Toporov, "Effect of contact deformations on the adhesion of particles," Journal of Colloid and Interface Science, 53(2), 314-26 (1975).

[11] D. S. Grierson, E. E. Flater, and R. W. Carpick, "Accounting for the JKR - DMT transition in adhesion and friction measurements with atomic force microscopy," Journal of Adhesion Science and Technology, 19, 291 (2005).

[12] Z. Zheng, and J. Yu, "Using the Dugdale approximation to match a specific interaction in the adhesive contact of elastic objects," Journal of Colloid and Interface Science, 310(1), 27-34 (2007).

[13] R. W. Carpick, N. Agraït, D. F. Ogletree *et al.*, "Measurement of interfacial shear (friction) with an ultrahigh vacuum atomic force microscope," Journal of Vacuum Science and Technology B, 14, 1289-1295 (1996).

[14] R. W. Carpick, N. Agraït, D. F. Ogletree *et al.*, "Erratum:Measurement of interfacial shear (friction) with an ultrahigh vacuum atomic force microscope," Journal of Vacuum Science and Technology B, 14, 2772 (1996).

[15] D. Maugis, "Adhesion of spheres: The JKR-DMT transition using a dugdale model," Journal of Colloid and Interface Science, 150(1), 243-269 (1992).